J. Am. Chem. Soc. **1986**, *108*, 6168–6173

Conformational Energy Calculations and Proton Nuclear Overhauser Enhancements Reveal a Unique Conformation for Blood Group A Oligosaccharides

C. Allen Bush,* Zhen-Yi Yan, and B. N. Narasinga Rao

Contribution from the Department of Chemistry, Illinois Institute of Technology, Chicago, Illinois 60616. *Received March 17, 1986*

Abstract: The ^1H NMR spectra of a series of blood group A active oligosaccharides containing from four to ten sugar residues have been completely assigned, and quantitative nuclear Overhauser enhancements (NOE) have been measured between protons separated by known distances within the pyranoside ring. The observation of NOE between anomeric protons and those of the aglycon sugar as well as small effects between protons of distant rings suggests that the oligosaccharides have well-defined conformations. Conformational energy calculations were carried out on a trisaccharide, Fuc(α-1→2)[GalNAc(α-1→3)]-Galβ-O-me, which models the nonreducing terminal fragment of the blood group A oligosaccharides. The results of calculations with three different potential energy functions which have been widely used in peptides and carbohydrates gave several minimum energy conformations. In NOE calculations from conformational models, the rotational correlation time was adjusted to fit T_1's and intra-ring NOE. Comparison of calculated maps of NOE as a function of glycosidic dihedral angles showed that only a small region of conformational space was consistent with experimental data on a blood group A tetrasaccharide alditol. This conformation occurs at an energy minimum in all three energy calculations. Temperature dependence of the NOE implies that the oligosaccharides adopt single rigid conformations which do not change with temperature. Since the glycosidic linkage of GalNAc(α1→3)Gal-β adopts an unusual conformation in which the anomeric proton is closer to Gal H4 than it is to Gal H3, some caution should be used in the application of recently proposed 2-D NMR methods which use NOE to determine the positions of intersaccharide linkage in oligosaccharides. While the results of the conformational energy calculations are very sensitive to the details of the nonbonded interactions, the influence of electrostatics, hydrogen bonding, and torsional potentials is minimal.

I. Introduction

In recent years a number of conformational studies on the complex oligosaccharides of glycoproteins and glycopeptides have appeared. Brisson and Carver[1,2] have used proton NMR to study the conformation of the *N*-asparagine linked complex and high mannose glycopeptides with special emphasis on the conformation of the oligomannosides.[3] Paulsen et al.[4,5] have reported conformational energy calculations and proton nuclear Overhauser enhancements (NOE) on a series of synthetic oligosaccharides closely related to the *N*-asparagine linked glycopeptides. The general conclusion reached by both research groups was that the conformations about the 1→2, 1→3, and 1→4 glycosidic linkages in these glycopeptides show well-defined conformations which lie at minima in the conformational energy space. The Man(α-1→-6)Man linkage, which occurs as a branch point in these glycopeptides, is a special case as a result of the rotation of three single bonds leading to greater flexibility. Although definitive conclusions about the precise dihedral angles of this 1→6 linkage remain controversial, its conformation has been proposed to be especially important due to the threefold barrier to rotation about the C5–C6 bond.[2]

The nonreducing terminal blood group active fragments found on mucin type glycoproteins have been studied by Lemieux et al.[6] by conformational energy calculations as well as by proton NMR spectroscopy. They have suggested that these oligosaccharides also adopt single well-defined low-energy conformations. In most cases, reducing terminal core structures of these blood group oligosaccharides are attached to peptide by -*O*-glycosidic linkages between α-GalNAc and serine or thronine. The conformation of the core structure of these "mucin" type glycopeptide linkages has been studied by Bush and Feeney,[7] who used the antifreeze glycoprotein of polar fish as a model glycopeptide.

The research methodology used in the studies cited above, which includes measurement of proton NOE and coupling constants, is similar to that used in peptide conformational studies. The methods for conformational energy calculation are also similar and are derived in most cases from methods first developed for study of peptide conformation. Despite the similarity in experimental and computational methodology, there are some substantial differences in the conclusions which result from the peptide and oligosaccharide research. Single well-defined conformations appear much more commonly in complex oligosaccharides. Single rigid conformations are rare for peptides except in the case of cyclic structures with severe steric hindrance. A related observation is that nonbonded interactions dominate in the energy calculations on most oligosaccharides. The HSEA (hard-sphere exoanomeric effect) method, used successfully by Lemieux and co-workers and by Paulsen et al.,[4,5] includes only nonbonded interactions. Rao et al.[8] have proposed that the observation in blood group H oligosaccharides that the conformations do not seem to depend strongly on temperature may result from the predominance of repulsive nonbonded interactions. An additional difference between the practice of peptide and oligosaccharide conformational research is that NOE are even more useful in the latter than the former system. Since numerous carbon-bound protons in carbohydrates contribute to the relaxation, proton dipolar interaction predominates and large NOE are seen between protons on adjacent residues while smaller ones have often been observed for next-nearest neighboring residues.[8] An important parameter in NOE and T_1 phenomena is the rotational correlation time, which is longer for oligosaccharides in D_2O than for a peptide of the same molecular weight. An additional difference is that, in spite of the small dependence of oligosaccharide conformation on temperature, the τ_c of oligosaccharides depend more strongly on temperature than for the case of peptides.[8]

Much has been learned in the years of study of peptide conformation by conformational energy calculation, X-ray crystal-

(1) Brisson, J. R.; Carver, J. P. *Biochemistry* **1983**, *22*, 3671–3680.
(2) Brisson, J.-R.; Carver, J. P. *Biochemistry* **1983**, *22*, 3680–3686.
(3) Brisson, J.-R.; Carver, J. P. *Biochemistry* **1983**, *22*, 1362–1368.
(4) Paulsen, H.; Peters, T.; Sinnwell, V.; Lebuhn, R.; Meyer, B. *Liebigs Ann. Chem.* **1984**, 951–976.
(5) Paulsen, H.; Peters, T.; Sinnwell, V.; Lebuhn, R.; Meyer, B. *Liebigs Ann. Chem.* **1985**, 489–509.
(6) Lemieux, R. U.; Bock, K.; Delbaere, L. T. J.; Koto, S.; Rao, V. S. R. *Can. J. Chem.* **1980**, *58*, 631–653.
(7) Bush, C. A.; Feeney, R. E. *Int. J. Peptide Protein Res.*, in press.
(8) Rao, B. N. N.; Dua, V. K.; Bush, C. A. *Biopolymers* **1985**, *24*, 2207–2229.

0002-7863/86/1508-6168$01.50/0

lography, and NMR spectroscopy. The resulting knowledge about the relation between structure and conformation of polypeptides is now finding use in the genetic engineering of enzymes, hormones, and other bioactive peptides. Since much less is known about the conformation of complex carbohydrates, few reliable generalizations are possible. But conformational generalizations about complex oligosaccharides should become useful as their functional roles become better understood. The conformations of the complex oligosaccharides of glycoproteins and glycolipids play an important role in their biosynthesis, degradation, and function as lectin and immunological receptors.

II. Materials and Methods

A. NMR Experiments. ^{1}H NMR spectra were recorded on a Nicolet NT-300 spectrometer equipped with a 293C pulse programmer. The isolation of the blood group A oligosaccharide alditols from ovarian cyst mucin glycoproteins by high-pressure liquid chromatography has been described previously. The complete assignment of their proton NMR spectra has been made by 2-D COSY and 1-D spin difference decoupling with spin simulation.[9] For quantitative measurement of the NOE, a 3-s presaturation was followed by a 90° acquisition pulse with the decoupler off. The decoupler power and frequency were varied in small increments at the saturated resonance to evaluate the effects of cross-saturation and incomplete saturation. Enhancements were obtained by scaled subtraction of the irradiated spectrum from the control or alternatively by integration of the difference spectra. Proton T_1's were measured by the inversion recovery method with fitting of the peak intensities to a single exponential decay.

B. Conformational Calculations. For molecular modeling of the disaccharide and trisaccharide fragments of blood group A oligosaccharides, atomic coordinates of the monosaccharide subunits were taken from crystallographic data.[10,11] Pyranosides were held fixed in the normal chair conformation, and the conformational energy was calculated as a function of the glycosidic dihedral angles Φ and Ψ. The glycosidic dihedral angle Φ is defined by the four atoms O_{ring}–C1–O1–C_x, and Ψ is defined by C1–O1–C_x–C_{x-1} with right handed rotations taken as positive dihedral angles following the IUPAC convention.[12] The glycosidic bond angles were set at 117°.

Energies of the oligosaccharides were calculated as a function of the glycosidic dihedral angles with use of three different sets of empirical energy functions, each of which has been used in previous studies of carbohydrate conformations. The functions of Momany et al.[13] have been used previously in this laboratory.[14] In this method, nonbonded interactions are computed with use of Lennard-Jones 6–12 potential functions with parameters determined by fitting to crystal structure data.[15] This method, hereafter referred to as M&S, also includes electrostatic effects calculated by monopoles or partial charges calculated for each atom by the semiempirical CNDO/2 method. A special 10–12 hydrogen bonding function was substituted for the 6–12 function to simulate the hydrogen-bonding interactions.[15] A simple threefold torsional potential is included in this method with U_0 = 0.6 kcal/mol for rotation about C–O bonds.

A slightly different set of empirical potential functions in the CAMSEQ or Chemlab computer software[16,17] has also been used for conformational energy calculation on oligosaccharides.[18] In this method, referred to as Hop, the nonbonded interactions are represented by Lennard-Jones 6–12 functions but with parameters which differ from those of M&S. The electrostatic interactions are calculated by the same method as in M&S, but the hydrogen-bonding function and torsional potential differ.[17]

Table I. Experimental Nuclear Overhauser Effect (NOE) Data at 24 and 60 °C

saturated resonance	obsd resonance	NOE (%) 24 °C	NOE (%) 60 °C
GalNAc H1	GalNAc H2 + Gal H4	20*[a] (±2)	29* (±2)
	GalNAc H2	12 (±3)	19 (±3)
	Gal H3	3 (±2)	2 (±2)
Fuc H1	GalNAc H5	2 (±2)	2 (±2)
	Fuc H2	11 (±3)	14 (±3)
	Gal H2 + GalNAc H3	13* (±2)	20* (±2)
	GalNAc H3	4 (±2)	n.a.[b]
Gal H1	GalNAcol H3	5 (±2)	9 (±2)
	Gal H3	3 (±2)	5.5 (±2)
	Gal H5	6 (±2)	9 (±2)

[a] The percentage NOE marked with an asterisk is the sum of the NOE due to the various overlapping resonances. [b] n.a. indicates the value is not available due to overlap of resonances.

Table II. Experimental Spin-Lattice Relaxation Time (T_1) Data at 24 and 60 °C

obsd resonance	T_1 (ms) 24 °C	T_1 (ms) 60 °C
Fuc H1	441 (±30)	590 (±30)
GalNAc H1	465 (±30)	565 (±30)
Gal H1	330 (±30)	360 (±30)

The HSEA (hard sphere exoanomeric effect) method was introduced by Lemieux et al.[6] especially for use with carbohydrates. The nonbonded interactions are represented by Kitaigorodsky 6-exp potential functions with the parametrization of Venkatachalam and Ramachandran.[19] In the HSEA method, a torsional potential called the "exo-anomeric effect"[20] for rotation about the dihedral angle Φ is deduced from vacuum quantum mechanical calculations on dimethoxymethane.[21] No provision for torsional potentials about Ψ, for electrostatic energies, or for hydrogen-bonding effects is included. In HSEA calculations, the methyl and hydroxymethyl groups are treated as single lumped atoms, and hydrogen atoms of hydroxyl groups are ignored.

In the interpretation of experimental NMR data, we have attempted to quantitatively reconcile the NOE with calculated conformations using a method suggested by Brisson and Carver.[3] For carbohydrates, in which proton relaxation is predominantly by proton dipole–dipole interaction,[3] eq 3.6 from Noggle and Schirmer[22] gives $f_d(s)$, the steady-state NOE at the resonance of proton d on saturation of the resonance of proton s.

$$f_d(s)R_d = \sigma_{ds} - \sum_n \sigma_{dn} f_n(s) \quad (1)$$

In eq 1 R_d is $1/T_1$ for the observed resonance, d, and the σ are the proton–proton dipole cross-relaxation terms. Since for large oligosaccharides the extreme narrowing assumption is not valid, R_d and σ depend on τ_c and the spectrometer frequency, ω, as well as on the inverse sixth power of the distance between the protons.

$$R_d = \left(\frac{\mu_0}{4\pi}\right)^2 \frac{\gamma^4 \hbar^2}{10} \sum_{i \neq j} \frac{\tau_c}{r_{ij}^6} \left(\frac{3}{1 + \omega^2 \tau_c^2} + \frac{6}{1 + 4\omega^2 \tau_c^2} + 1 \right) + \rho_d^* \quad (2)$$

$$\sigma_{ij} = \left(\frac{\mu_0}{4\pi}\right)^2 \frac{\gamma^4 \hbar^2}{10} \frac{\tau_c}{r_{ij}^6} \left(\frac{6}{1 + 4\omega^2 \tau_c^2} - 1 \right) \quad (3)$$

The sum over all the NOE on the right side of eq 1 implies a set of coupled equations. As a result of the multitude of carbon bound protons contributing to the relaxation in carbohydrates, it is often the case that

(9) Dua, V. K.; Rao, B. N. N.; Wu, S. S.; Dube, V. E.; Bush, C. A. *J. Biol. Chem.* **1986**, *261*, 1599–1608.
(10) Longchambon, P. F.; Ohannessian, J.; Avenel, D.; Neuman, A. *Acta Crystallog. B31*, **1975**, 2623–2627.
(11) Arnott, S.; Scott, W. E. *J. Chem. Soc., Perkin Trans. 2* **1971**, 324–335.
(12) IUPAC-IUB Commission on Biochemical Nomenclautre: *Euro. J. Biochem.* **1983**, *131*, 5–7.
(13) Momany, F. A.; McGuire, R. F.; Burgess, A. W. Scheraga, H. A. *J. Phys. Chem.* **1975**, *79*, 2361–2381.
(14) Bush, C. A. *Biopolymers* **1982**, *21*, 535–545.
(15) Momany, F. A.; Carruthers, L. M.; McGuire, R. F.; Scheraga, H. A. *J. Phys. Chem.* **1974**, *78*, 1595–1620.
(16) Hopfinger, A. J. *Conformational Properties of Macromolecules*; *Academic*: New York, 1973, Molecular Biology Services.
(17) Potenzone, R.; Cavicchi, E.; Weintraub, H. J. R.; Hopfinger, A. J. *Comput. Chem.* **1977**, *1*, 187–194.
(18) Potenzone, R.; Hopfinger, A. J. *Polymn. J.* **1978**, *10(2)*, 181–199.
(19) Venkatachalam, C. M.; Ramachandran, G. N. In *Conformation of Biopolymers*; Ramachandran, G. N.; Ed.; Academic: New York, 1967; Vol. 2, p 87.
(20) Thogersen, H.; Lemieux, R. U.; Bock, K.; Meyer, B. *Can. J. Chem.* **1982**, *60*, 44–57.
(21) Jeffrey, G. A.; Pople, J. A.; Binkley, J. S.; Vishveshwara, S. *J. Am. Chem. Soc.* **1978**, *100*, 373–379.
(22) Noggle, J. H.; Schirmer, R. E. *The Nuclear Overhauser Effect*; Academic: New York,, 1971.
(23) Lipkind, G. M.; Verovsky, V. E.; Kochetkov, N. K. *Carbohydr. Res.* **1984**, *133*, 1–13.

one or more terms make significant contributions to the sum in eq 1 and the entire set of equations must be solved simultaneously. The physical interpretation of this phenomenon, which causes the "three spin effect" discussed by Noggle and Schirmer,[22] is that a proton which has large NOE on irradiation of one of its neighbors in turn influences the relaxation of a third resonance. Both NOE and the proton T_1 were calculated from eq 1 with use of computer generated models in which the glycosidic dihedral angles were systematically varied to give maps of NOE and T_1 as a function of oligosaccharide geometry. Then those conformations whose calculated NOE and T_1 were consistent with our experimental data were mapped. The calculated NOE and T_1's were compared with experimental data, and contour maps were generated that display the angles for which the calculated value fell within the error bounds of the observed values. The range of glycosidic dihedral angles consistent with the experimental values can be found by the area of intersections of the maps for different experimental measurements of NOE and T_1's. This method is especially useful for interpretation of the small (2–3%) NOE which we have observed between protons of residues separated by more than one glycosidic bond.

III. Results and Discussion

1. Experimental NMR Results. The NOE observed at 24 and 60 °C for the blood group A tetrasaccharide (R6) are given in

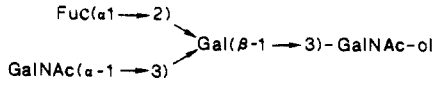

R6

Table I, and T_1 data for the anomeric protons are given in Table II. Since our interpretation of these data is quantitative, a discussion of the error limits given in Table I is in order. The errors are of two types. The noise level in the control and irradiated spectra contributes a constant level of uncertainty which is most significant for small NOE. For the data of Table I the noise level is about 1% so this is the smallest NOE to which any significance can be attached. A second source of error results from uncertainty in the level of saturation of a resonance and the effect of spill-over saturation of neighboring resonances in the spectrum. This error is proportional to the size of the NOE and is most important in the larger enhancements. Measurements of NOE for saturation of an isolated resonance as a function of saturating decoupler power indicate that measured NOE does not vary significantly in the range of 80 to 100% saturation, but a decrease in the measured NOE of approximately 20% is seen with 60% saturation. Spill-over saturation for resonances 20–40 Hz removed from the irradiated resonance is serious with 100% saturation but much less so at 60–80% saturation. We conclude from these experiments that for lines such as the 3-Hz doublets of the α anomeric proton resonances, errors due to spill-over saturation are not unavoidable for resonances 40 Hz apart and that semiquantitative NOE can be determined for resonances separated by as little as 20 Hz.

At 24 °C, saturation of Fuc H1 resulted in 11% NOE at Fuc H2 and a total of 13% at the partially overlapping resonances of Gal H2 (3.902 ppm) and GalNAc H3 (3.930 ppm). A small effect was also observed at GalNAc H5. The individual NOE at Gal H2 and GalNAc H3 reported in Table I were determined by integrating the isolated half of the multiplet of the GalNAc H3 and subtracting twice that value from the total integral of the overlapping resonances in the difference spectrum. This procedure was verified by spectral simulation. This procedure could not be used to separate these NOE in the 60 °C spectrum because the overlap of the GalNAc H3 and Gal H2 resonances was more severe.

On saturation of GalNAc H1, GalNAc H2 (4.247 ppm) and Gal H4 (4.225 ppm) showed a combined NOE of 20% while Gal H3 (aglycone proton) showed 3%. The effects at Gal H4 and GalNAc H2 were separately determined by curve decomposition with use of the known multiplet structures as described above. Saturation of Gal H1 gave NOE at the two syn axial protons, H3 (3%) and H 5 (6%).

The higher NOE at 60 °C results from the dependence of the rotational correlation time, τ_c, on temperature. This effect results from decreased water binding to the oligosaccharide at the higher temperature rather than from a change of conformation of the oligosaccharide with temperature as is shown by the constancy of the ratio of inter- to intraring NOE.[8]

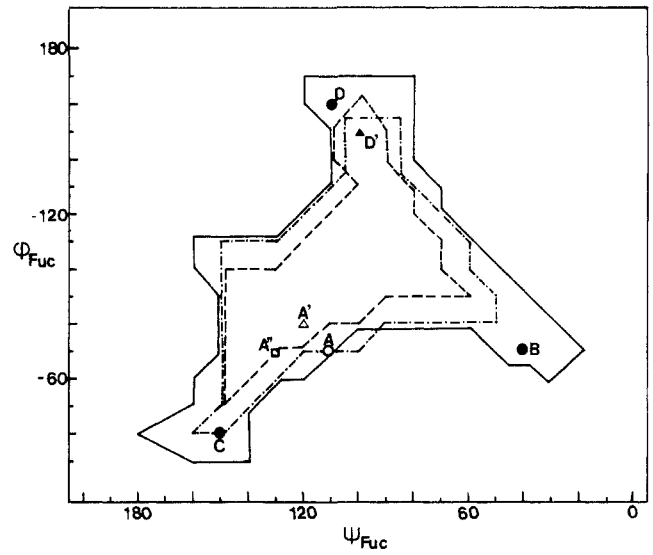

Figure 1. Nonbonded energy for Fuc(α1→2)Galβ-O-methyl as a function of the glycosidic dihedral angles Φ_{Fuc} and Ψ_{Fuc}. Contours at 4 kcal/mol above the minimum are drawn for the method of M&S (– – –), Hop (—), and HSEA (–·–). The open circle is the global minimum for Hop, and the filled circles are other local minima. Squares represent results with HSEA, and triangles are results for M&S.

NOE data have been measured for a number of larger oligosaccharides ranging up to a decasaccharide whose structures were determined by Dua et al.[9] The cores of these oligosaccharides include both type 1 and type 2 chains all having the nonreducing terminal blood group A terminal fragment, Fuc(α1→2)[GalNAc(α1→3)]Galβ-O-. In all cases, the NOE data for these nonreducing terminal residues was similar to those reported for R6 in Table I.

2. Empirical Energy Calculations. For the disaccharide, Fuc(α1→2)Galβ-O-methyl, the energy was calculated as a function of the two glycosidic dihedral angles, and the disaccharide energy map in Figure 1 shows the nonbonded part of the energy with the three methods M&S, Hop, and HSEA which were defined above. Two low-energy minima were found with the method M&S where D' in Figure 1 is 2.1 kcal/mol higher than A'. Using the method of Hop, four low-energy minima were found with B and C at 0.5 kcal, and D at 0.7 kcal above the global minimum at A. A single energy minimum (at A") was found by using HSEA. The greater area enclosed by the 4-kcal contour for the Hop method in Figure 1 shows that this potential energy function is more "flexible" than the other two. The greater "rigidity" of the M&S potential energy functions arises from the larger van der Waals radii of the atoms; the r_0^{kk} are significantly larger than those in Hop.

Although provisions for electrostatic, torsional, and hydrogen bonding functions in the M&S and the Hop methods are available, their inclusion has a minimal effect on the shape of the maps and the number and positions of the local minima. The differences in electrostatic contributions to the conformational energy among the four local minima of the Hop method (Figure 1) were less than 0.3 kcal/mol. The contribution of the torsional terms to the calculated energy were slightly more significant. The torsional energy for conformations A' and D' were the same with the M&S method. In the Hop method, the torsional energy of conformation B was 1.2 kcal lower than that of conformation A, making the former the global minimum when the torsional term was included. The electrostatic and hydrogen bonding terms make contributions which are less than the anticipated error of any of the empirical energy methods. The torsional terms make small but significant (1–2 kcal) contributions in each method. But since the torsional potentials differ qualitatively for all three methods and their basic theoretical justifications are weak, it is difficult to evaluate the

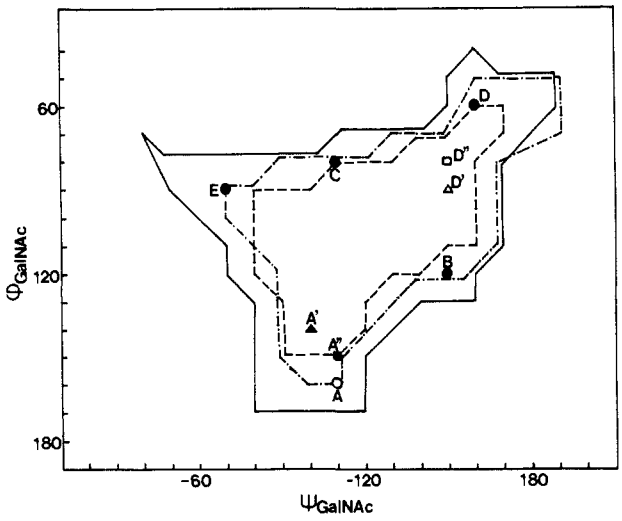

Figure 2. Nonbonded energy for GalNAc(α1→3)Galβ-O-methyl as a function of the glycosidic dihedral angles Φ_{GalNAc} and Ψ_{GalNAc}. Contours at 4 kcal/mol above the minimum are drawn for the method of M&S (---), Hop (—), and HSEA (-·-). The open circle is the global minimum for Hop, and filled circles are other minima. Squares represent results for HSEA and triangles for M&S.

reliability of the torsional terms.

Figure 2, which gives the map of the nonbonded energy for the disaccharide GalNAc(α1→3)Galβ-O-methyl, illustrated the more "flexible" nature of the Hop functions compared to those of M&S. The area enclosed by the 4-kcal contour is larger for the former method. Of the five minima found with Hop, A and B in Figure 2 are nearly equal in energy with C at 0.8 kcal higher, D 1.3 kcal higher, and E 1.8 kcal/mol higher. The M&S method gives two minima with A' 1.1 kcal higher than D'. Two local minima were found with HSEA and A" 2.2 kcal above D". The nonbonded energy calculations give different answers depending on method, with Hop, M&S, and HSEA predicting different lowest energy conformations.

The addition of the electrostatic potential energies to the M&S and Hop methods did not result in any significant change in the ordering of the energy minima of Figure 2. But addition of torsional energies caused more significant changes in the result. Addition of the torsional energy to the results of M&S increased the difference between A' and D' to 1.6 kcal/mol. In Hop calculations, the addition of torsional energy made conformation D the global minimum and conformation A was 0.7 kcal/mol higher. The conformations B, C, and E were about 1.3 kcal/mol above the minimum. The addition of torsion to the angle Φ in HSEA (the "exoanomeric effect") increased the energy of A" to 2.6 kcal/mol above the minimum at D".

Under the plausible assumption that the only strong interactions between residues which are not covalently linked should be repulsive, the glycosidic dihedral angles of the disaccharide which gave energies within 4 kcal/mol of the global minima were selected for use in four dimensional energy calculations for the trisaccharide, Fuc(α1→2)[GalNAc(α1→3)]Galβ-O-methyl. From the results of these calculations, some selected typical conformations representing distinct energy minima are presented in Table III. The global minima calculated by the methods Hop and HSEA are nearly the same while the energy of that minimum is 8.6 kcal above the global minimum in calculations by the method of M&S. The major contribution to the high energy of this conformation in M&S is the repulsive interaction of O2 of fucose with O3, O4, and H5 of GalNAc. The size of this repulsion is enhanced in M&S calculations as a result of the larger atomic radii (r_0^{kk}) in that method. Since the different methods gave different low-energy conformations, it is difficult to judge what is the conformation, if needed there is a unique fixed conformation. An independent approach to this problem is to use NOE and T_1 calculations as a function of conformation and compare them to our experimental data.

Table III. Selected Distinct Minima Calculated by Three Methods

	conformational angles				
	fucose		GalNAc		rel energy
conformer	ϕ	ψ	ϕ	ψ	(kcal/mol)
(a) M&S					
F1	-100	70	110	-150	0.00
F2	-100	80	150	-100	1.39
F3	-100	90	60	-170	6.10
F4	-60	140	60	-170	7.23
(b) Hop					
A1	-80	100	60	-160	0.00
A2	-80	50	50	-160	0.71
A3	-150	80	60	-160	1.53
A4	-80	100	100	-160	4.96
A5	-140	90	120	-160	3.52
A6	-60	130	50	-160	1.96
(c) HSEA					
K1	-80	100	60	-170	0.00
K2	-60	140	60	-170	0.58
K3	-70	130	150	-110	1.77

3. Calculation of NOE and T_1. As a result of the importance of the terms in ω and τ_c in eq 1, 2, and 3, an estimate of the latter parameter is necessary for calculation of the NOE and T_1. In our studies this parameter was determined by two independent methods. The first method used was to correlate experimental values of ^{13}C T_1 with τ_c. (The unpublished T_1 data were provided by Dr. T. Gerken.) The second method was to adjust τ_c in the calculation to a value which gave the experimental NOE values for proton pairs for which the NOE did not depend strongly on conformation. NOE for protons whose distances were held fixed in the pyranoside chair and whose T_1's were insensitive to conformation include that at Fuc H2 on saturation of Fuc H1 and that at GalNAc H2 on saturation of H1. Both methods gave τ_c between 0.2 and 0.4 ns for the tetrasaccharide R6.

Equations 2 and 3 show that if ω is near τ_c, even a small change in τ_c has an important influence on the calculated NOE. However, the calculated ratio of two NOE does not depend nearly so strongly on the choice of τ_c. Therefore, the relative NOE, the ratio of an interring to an intraring NOE, was used in our data analysis following Brisson and Carver.[3]

The experimental NOE reported in Table I can be divided into three categories. The computed values of NOE with eq 1 of one group of NOE (e.g. the effect at the resonance of Gal H2 on saturation of Fuc H1) depend mainly on the value of the dihedral angles of the fucosidic linkage while the computed values of a second group of NOE (e.g., the effect at Gal H4 on saturation of GalNAc H1) depend mainly on the conformation of the linkage between GalNAc and Gal. For these two groups of NOE the conformation of one of the glycosidic linkages can be held fixed at some reasonable value and the NOE computed as a function of the dihedral angles of the other glycosidic linkage. Thus two-dimensional maps of computed NOE as a function of conformation at 10° intervals were calculated for comparison with the experimental data. For a third group of NOE data (e.g., NOE at the resonance of GalNAc H3 on saturation of Fuc H1), two-dimensional mapping was impossible due to the dependence of the computed NOE on all four dihedral angles.

Figure 3 shows a map of the regions in which the NOE and T_1 computed as a function of the conformation of the GalNAc-(α1→3)Gal glycosidic linkage agree with the experimental data given in Table I. In Figure 3 the cross-hatched area in the conformational map in which the computed NOE and T_1 agree with experimental values is small and corresponds to the local energy minimum region marked D in Figure 2. In the data of Figure 4, the region of the conformational map for the fucosidic linkage showing agreement of the calculated and experimental NOE and T_1 is quite limited and corresponds to the region of minimum energy marked A in Figure 1.

Finally the conformations of the two glycosidic linkages in the small allowed regions of Figures 3 and 4 were searched in a

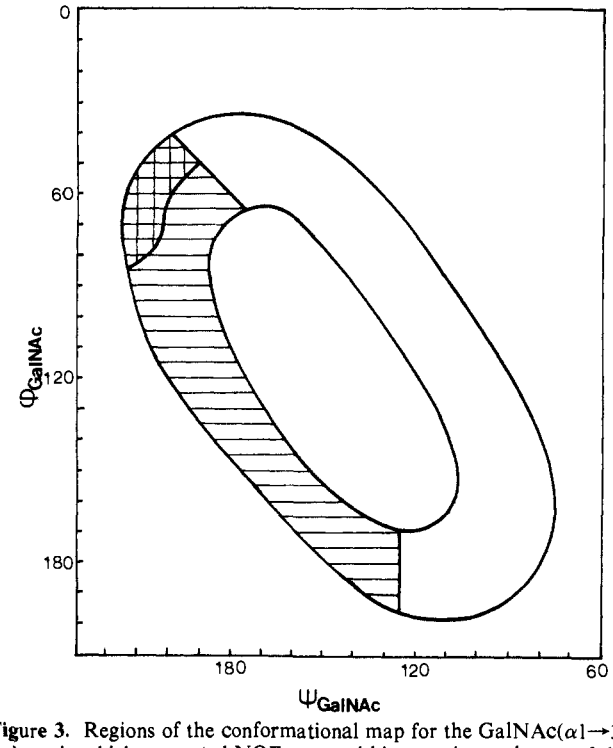

Figure 3. Regions of the conformational map for the GalNAc(α1→3) linkage in which computed NOE agree within experimental error of the values in Table I. The full circle is the region of agreement for the ratio of NOE at Gal H4 to that at GalNAc H2 on saturation of GalNAc H1, and in the lined region, the ratio of NOE at Gal H3 to that at GalNAc H2 also agrees. The cross-hatched region is that in which the computed value of T_1 of GalNAc H1 also agrees with the data of Table II.

Table IV. Conformations Consistent with Observed NOE[a] and T_1[b]

fucose		GalNAc		calcd T_1 (ms) at 24 °C		
ϕ	ψ	ϕ	ψ	Fuc H1	GalNAc H1	Gal H1
-60	130	50	-160	424	452	376
-70	130	50	-160	437	452	380
-80	130	50	-160	434	452	383

[a] See Table I for a list of observed NOE. [b] See Table II for observed T_1.

four-dimensional space for agreement of the calculated NOE with the experimental NOE of the third group. That group of NOE data includes the enhancement at GalNac H3 and H5 on saturation of Fuc H1 whose computed values depend on the conformation of both glycosidic linkages. In Table IV are listed those conformations of the trisaccharide fragment Fuc(α1→2)[GalNAc(α1→3)]Galβ-O-methyl for which all the calculated NOE and T_1's agree with experimental data. We conclude that for only a very limited range of conformations are the computed NOE and T_1 data consistent with the experimental data.

The calculated T_1 data in Table IV are consistent with the experimental values in Table II at 24 °C for Fuc H1 and GalNac H1, but those calculated for Gal H1 are larger than the experimental values. The reason for the discrepancy lies in the difference between our computational model, a β-O-methyl galactoside and the experimental compound, R6, a tetrasaccharide alditol. In the experimental compound, there are more protons near β Gal H1 than in the computational model.

The conformational energy calculations give several different candidates for the lowest energy conformation. It is not clear which is correct or whether a conformational average exists. But the NOE data of Table I show bigger effect at Gal H4 than at Gal H3 on saturation of GalNAc H1, suggesting that the distance between GalNAc H1 and Gal H4 is shorter than Gal H3, a situation which is true for conformations in the D area of Figure 2. This important fact will be quantitatively interpreted in our discussion of NOE interpretation below.

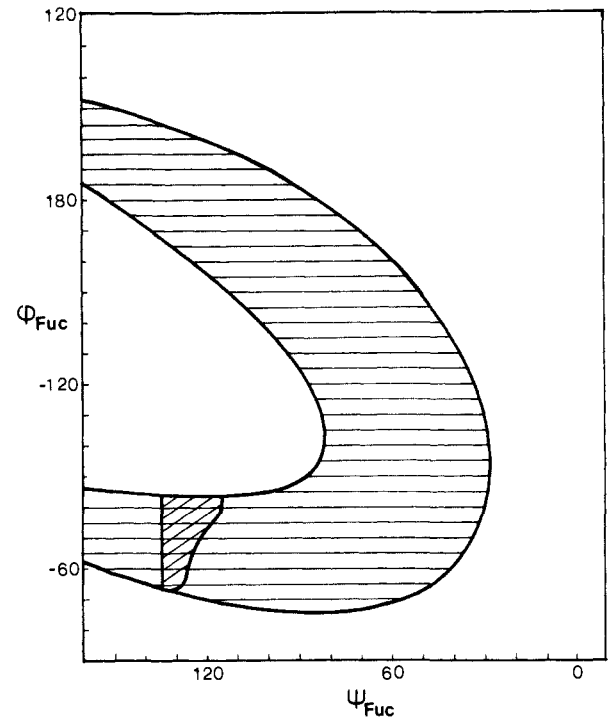

Figure 4. Regions of the conformational map for the Fuc(α1→2) linkage in which computed NOE agree within experimental error of the values in Table I. The large enclosed region is that in which the ratio of the NOE at Gal H2 to that at Fuc H2 on saturation of Fuc H1 agrees with experiment at the smaller cross-hatched region in which the computed value of T_1 of Fuc H1 agrees with experimental value in Table II.

IV. Conclusions

The NOE and T_1 calculated from model conformations agree within the error limits of the experimental data only for a small range of conformational space. (See Figures 3 and 4). Although it is conceivable that the observed experimental result could arise from averaging over several conformations, that seems quite unlikely. The NOE observed at the proton resonances of the GalNAc residue on irradiation of Fuc H1 implies that rotation about both the fucose and GalNAc glycosidic bonds is restricted. Therefore, it is our interpretation that the blood group A trisaccharide fragment adopts a relatively rigid conformation close to that indicated in Table IV.

Although there are significant differences among the results of the conformational energy calculations by the three different methods described, all three have a local minimum near the conformation which is consistent with the NMR data. We conclude from this result that conformational energy calculations based on empirical energy functions are inadequate to accurately predict the conformation of at least some complex oligosaccharides. It is possible that certain of the assumptions inherent in the use of empirical energy functions are not rigorously correct. The three methods tested in this work gave qualitative or semiquantitative agreement, but we believe that there is an uncertainty level of several kcal/mol in the calculated energy. NMR methods provide a valuable adjunct which may resolve such ambiguities in cases such as the blood group A oligosaccharides.

Since empirical methods arbitrarily divide the energy into contributing terms, one may ask which are the most important. In agreement with the results of others,[23] this work indicates that the nonbonded interactions predominate in carbohydrate energy calculations. We find the contributions of the electrostatic charge terms and the hydrogen bonding functions to be small. Although we did not attempt to include any hydrophobic effects in the calculation, we anticipate that they would not make a significant contribution since hydrophobic contributions are usually not larger than electrostatic ones and the nonbonded energies make large contributions. The torsional terms can be of some importance, but the details of these functions are uncertain. For the car-

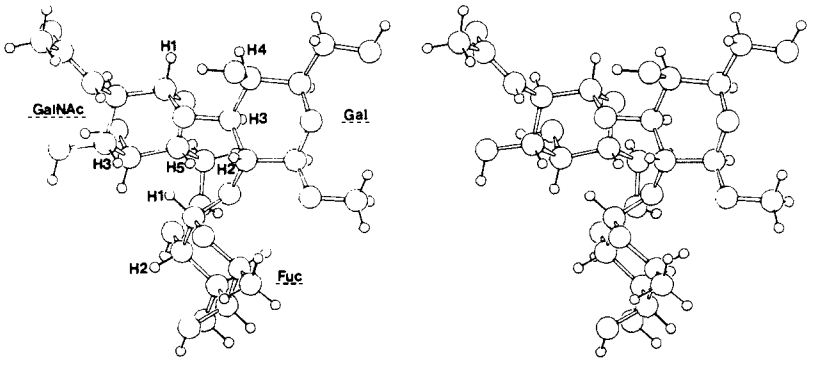

Figure 5. Stereodiagrams of trisaccharide for conformation A6 (see Table III), $\phi_{Fuc} = -60°$, $\psi_{Fuc} = 137°$; $\phi_{GalNAc} = 50°$, $\psi_{GalNAc} = -160°$.

Table V. Minimum Energy Conformations Calculated by 2° Intervals[a]

	conformational angles				
	fucose		GalNAc		rel energy
conformer	ϕ	ψ	ϕ	ψ	(kcal/mol)
(a) M&S					
F1M	-100	70	110	-150	0.0
F4M	-62	138	56	-174	5.1
(b) Hop					
A1M	-80	92	68	-154	0.0
A6M	-60	137	50	-160	1.9
(c) HSEA					
K1M	-84	92	64	-164	0.0
K2M	-62	140	58	-174	0.7

[a] From the global minima and conformations of Table III which most closely agree with the NOE results of Table IV.

bon–carbon single bond, a threefold potential barrier has been experimentally characterized in small molecule models, but for glycosidic or amide bonds the torsional barrier is small and not well understood. Lemieux et al.[6] and Torgerson et al.[20] have proposed the "exo-anomeric" effect, a torsional barrier about the angle Φ, but the theoretical basis for this function relies on just two calculated points in an ab initio calculation.[21] The "exo-anomeric" theory does not provide a torsional function for the glycosidic bond, Ψ.

As a result of the preponderant influence of the nonbonded interactions in carbohydrate conformational calculations, the results are extremely sensitive to the details of the parametrization as is illustrated in Figures 1 and 2. The M&S and Hop methods may be easily compared since they both use the same functional form (**6–12**) for nonbonded interactions. The M&S parameters, with larger atoms, result in a more restricted conformational space. Although this reduced flexibility is consistent with the rigid conformations deduced from our interpretation of the experimental NOE data (Figures 3 and 4), the M&S parameters make a prediction for the conformation about the GalNAc bond which is inconsistent with experiment. At the conformation of the global minimum in the M&S calculations, the NOE on irradiation of GalNAc H1 observed at Gal H3 is predicted to be larger than that at H4.

It was possible to find a conformation for the blood group A trisaccharide fragment which is consistent simultaneously with the experimental NOE data and the energy calculations. The local minima, F4, A6, and K2 of Table III, are all near the conformation which is consistent with the NMR data. Energy minima based on 2° intervals were calculated for these three conformations and for the global minima F1, A1, and K1 of Table III. In the results in Table V, the method of M&S gives conformation F4M which is 5.1 kcal above the global minimum while the Hop and HSEA methods give local minima consistent with the NOE and which are not far from the global energy minima. Although the minimized conformation A6M (Table V) from Hop was selected as the most likely one, the errors on the dihedral angles should be considered ±5°. This conformation is similar to that originally proposed for blood group A oligosaccharides by Lemieux et al.[6] In this conformation, which is illustrated in the stereopair of Figure 5, one can see that GalNAc H1 is closer to Gal H4 than it is to Gal H3 (the aglycon proton). Also, Fuc H1 is close to GalNAc H3 and H5 thus explaining the small NOE observed between next nearest-neighboring residues. The NOE and T_1 data for both the 24 and 60 °C experimental data fit this conformation with only a change in the τ_c. The conformation of this type of oligosaccharide does not depend strongly on temperature, and the change in rotational correlation time arises from a change in water binding.[8]

Acknowledgment. We thank Dr. T. Gerken of Case Western Reserve University for making available unpublished ^{13}C T_1 data on the tetrasaccharide. This research was supported by NIH Grant No. GM-31449.

Registry No. Fuc(α-1→2)[GalNAc(α-1→3)]Gal-β-O-Me, 103851-11-2.